Alkylation of Phenol: A Mechanistic View

Qisheng Ma, Deb Chakraborty, Francesco Faglioni, Rick P. Muller, and William. A. Goddard, III

California Institute of Technology, Pasadena, California 91125

Thomas Harris, Curt Campbell, and Yongchun Tang*

ChevronTexaco Energy Research and Technology Company, Richmond, California 94802

Received: October 20, 2005; In Final Form: December 12, 2005

The current work utilizes the ab initio density functional theory (DFT) to develop a molecular level of the mechanistic understanding on the phenol alkylation in the presence of a cation-exchange resin catalyst, Amberlyst-15. The catalyst is modeled with the benzene sulfonic acid, and the effect of this acid on olefins such as isopropene (*i*-Pr) and tributene (*t*-Bu) in a phenol solution mimics the experimental condition. A neutral-pathway mechanism is established to account for early-stage high concentration of the phenolic ether observed in experiments. The mechanism involves an exothermic reaction between olefin and the benzene sulfonic acid to form ester followed by three reaction pathways leading to direct O-alkylation, *o*-C-alkylation, and *p*-C-alkylation. Our calculations conclude that O-alkylation to form the phenolic ether is the most energetically favorable in the neutral condition. An ionic rearrangement mechanism describes intramolecular migrations of the alkyl group from the phenolic ether to form C-alkylphenols, while the positively charged protonation significantly lowers transition barriers for these migrations. The ionic rearrangement mechanism accounts for high yields of *o*-C-alkylphenol and *p*-C-alkylphenol. Competition between the H atom and the alkyl R group at the substitutive site of the protonated ortho configuration is found to be the determining factor to the ortho/para ratio of C-alkylation products.

1. Introduction

The alkylation of phenol with olefins in the presence of acid catalysts to produce alkylphenols has been subject of investigation for a long time because of its fundamental and industrial importance. Alkylated phenols are widely used as additives in gasoline, lubricants, and as hosts of consumer products. For instance, the *p*-alkylphenol isomer imparts improved performance properties to the class of metallic detergents used in lubricating oils, known as phenates. *tert*-Butyl-*iso*-octyl and *iso*-decyl phenols are widely used in the chemical industries as drilling oil additives, antioxidants, and polymer stabilizers.[1]

Both homogeneous and heterogeneous (solid) catalysts have been applied for the phenol alkylation. Homogeneous acid catalysts such as HF, H_2SO_4, $AlCl_3$, or BF_3 are commonly used, but the toxic aqueous waste resulting from catalysts remains problematic. On the other hand, uses of the eco-friendly heterogeneous catalysts such as macroporous cation-exchange resins (Amberlyst-15), NaX and Y zeolites, hetero polyacids, titania-supported $AlPO_4$, and silica-supported BF_3 have advanced in recent years. These heterogeneous catalysts are preferred to homogeneous acid catalysts since they can reduce the corrosiveness of the reaction compounds, are easily separated from the reactant−product mixture, and can eliminate undesirable side reactions.

The mechanistic understandings on these catalytic reactions, especially those at the atomic level, however, have not yet been fully obtained. To gain insights into the reaction mechanism occurring during the phenol alkylation in the presence of a cation-exchange resin catalyst, we have carried out a systematical theoretical study using the ab initio density functional theory (DFT). An overall phenol alkylation reaction can be described as a multistep process consisting of a neutral-pathway leading to the early O-alkylation, followed by a serial of ionic rearrangements resulting in the final C-alkylations. Details of these two mechanisms are presented herein with all stables, intermediates, and transition states computed.

Amberlyst-15, prepared by sulfonation of polystyrene cross linked with divinyl benzene, is a commonly used cation-exchange resin catalyst. For simplicity and cost-effectiveness, we modeled it with the benzene sulfonic acid as it shares the same functional group as Amberlyst-15. Two olefins, *iso*-propene (*i*-Pr) and *tri*-butene (*t-Bu*) are used in the present study to mimic the chemistry. Section 2 outlines the computational methodology, and section 3 describes the reaction mechanism by considering: (1) a neutral-pathway mechanism describes the direct phenol alkylation via a sulfonic ester complex, which leads to the early-stage ether formation, and (2) an ionic rearrangement mechanism for migrations of different alkyl groups migrating among substitutive sites on phenol to accomplish *o*- and *p*-C-alkylations. An overall discussion of the proposed mechanism is summarized in section 4.

2. Computational Details

The gas-phase geometries of reactants, products, intermediates, and transition states (TS) are fully optimized using the B3LYP flavor of density functional theory. This includes the

* To whom correspondence should be addressed. Mailing Address: Power, Environmental, and Energy Research Center (PEER) California Institute of Technology 738 Arrow Grand Circle Covina, CA 91722. E-mail Address: tang@peer.caltech.edu. Telephone: (626) 858-5077. Fax: (626) 858-9250.

10.1021/jp0560213 CCC: $33.50
Published on Web 01/24/2006

generalized gradient approximation (Becke nonlocal gradient correction), exact exchange using the Becke three-parameter exchange functional,[2] and the nonlocal correction functional of Lee, Yang, and Parr.[3] We have used the 6-31G(d) basis set for all out computations. This level of theory (B3LYP/6-31G(d)) has been recommended for providing a practical and reliable approach for the study of carbocation−aromatic ring interactions.[4] Particularly, since all compounds involved in our studies contain only C, H, O, S atoms, we anticipate that the effect of the basis set superposition error (BSSE) will be relatively small. All stationary points have positively identified for local minima (zero imaginary frequencies) and for TS (one imaginary frequency). Vibrational frequencies are also calculated at all stationary points to obtain zero-point energies (ZPE) and thermodynamic parameters.

In most experiments, a large excess of phenol is used and olefin is added with the sulfonic acid resin. Therefore, we consider phenol as the reaction solvent even in the presence of the heterogeneous catalyst. All gas-phase reactants, products, and transition geometries are recalculated in a dielectric continuum of phenol. The dielectric constant of $\epsilon = 12.4$ and a probe radius of $r_0 = 2.60$ Å are chosen for phenol. The solvent-phase energies of all of these species are obtained using the continuum−solvation technique[5−7] with the Poisson−Boltzmann (PB) approach[8] as integrated in the Jaguar quantum chemical program package.[9]

3. Results

3.1. Survey of Experimental Results.

Gas-phase chemistry of complexes of aromatic rings with carboncations is very rich because of the existence of both σ-complexes by reaction with the aromatic rings. A wealth of information on the relative energies of such areninum ions is found in the extensive gas-phase experimental work of Cacace et al.,[10] Kuck,[11] and Fornarini.[12] These studies used radiolytic techniques in conjunction with mass spectrometry to identify the gas-phase structure, stability of the gaseous cations, and mechanistic insight into many classes of aromatic reactions such as alkylation, nitration, and silylation.[12e] Furthermore, studies of rearrangement of the resulting carbonium ion such as toluenium or xylenium in gas as well as the solution phase have been reported.[13−15] However, detailed theoretical studies including characterization of TSs are very limited.[16] Semiempirical and ab initial studies of structures and energetic relations of some σ-complexes may be found in the literature.[17−22]

The early complexes could be π-complexes, H-bonded complexes, or ion-dipole complexes.[23−27] The existence of the intermediate π-complex in electrophilic aromatic substitution (EAS) in solution was originally proposed by Dewar.[28] The highest TS for such a reaction corresponding to a π-complex, the formation of which is considered to be rate determining.[29] The general consideration of such "cation−π interaction"[30,31] is relevant to enzymatic reactions,[32] η^6, η^2, and even η^1 complexes of aromatic ring with metal cations,[33] or with ammonium ions.[34−39] Formation of π-complexes in the reaction of carbocation with aromatic compounds in gas phase was first proposed by Grützmacher et al.[40] In contrast, very little information is available concerning the structure, energies of such π complexes of carbocation from theoretical point of view.[41−44]

Although a wealth of information and profound understanding of the gas-phase chemistry of EAS with carbocations has been extensively developed, we found only a single gas-phase experiment for the alkylation of phenol.[45] To develop basic understanding of the structure, energies, and plausible reaction pathway of alkylation of phenol, we attempted to simulate this experiment of Attina et al.[45]

TABLE 1: Relative Stabilization of Alkylated Phenols and Their Carbonium Ions in Both the Gas Phase and Phenol Solution[a]

	gas phase			in phenol		
	O-alkylation	C-alkylation		O-alkylation	C-alkylation	
alkyl	Oxo	ortho	para	oxo	ortho	Para
$C_2H_5^+$	14.98	4.17	0.00	15.05	4.58	0.00
C_2H_5	10.08	5.08	0.00	12.71	5.94	0.00
$C_3H_7^+$	9.55	4.81	0.00	10.82	6.70	0.00
C_3H_7	7.73	5.79	0.00	9.95	5.79	2.93
$C_4H_9^+$	4.54	4.14	0.00	6.87	5.70	0.00
C_4H_9	6.86	5.95	0.00	8.54	7.31	0.00

[a] All energies, in units of kcal/mol, are referred to their para isomers, which are the most energetically stable.

Tertiary butylation of phenol and anisole was carried out in the gaseous mixture of neopentane (720 Torr), small amount of aromatic substrates (phenol or anisole) (0.02−1.5 Torr), a radical scavanger O_2, and a gaseous base NH_3. The tertiary butyl cation was generated radiolytically from neopentane at 22 °C and thermally equilibrated by unreactive collisions with the neopentane molecules before attacking the aromatic ring. The oxonium or arenium ions formed the exothermic alkylation eventually transfer a proton to the gaseous base and the identity and yield of the neutral products were determined by gas−liquid chromatography. In solution the attack of a charged electrophile to the n-type (O-center) or π-type (aromatic ring) nucleophilic centers of phenol depends very much on the specific reaction environment, in particular on the solvation of the reagents and the charged intermediates. In contrast, the *tert*-butylation of phenol in gas phase occurs predominantly by the remarkably selective attack of t-$C_4H_9^+$ on the n-center yielding the O-alkylation ether as the major product. The thermodynamic stability of the oxonium ion was apparently considered responsible for such specificity of the reaction.

3.2. O-Alklation vs C-Alkylation.

Alkylation of phenol has an additional complication because of the possibility of the alkyl attacking to the phenolic oxygen (O-alkylation, or the oxo configuration) that leads to an ether formation beside desirable alkylations at the aromatic ring (C-alkylation). Indeed most experiments show evidences of a high initial-stage ether concentration.[46,47] O-Alkylated phenols also have numerous industrial applications, particularly in the production of dyes and agrochemicals.[48] However, the reactivity and the product selectivity of phenolic C-alkylation largely depend on olefins and the nature of catalysts. In the presence of heterogeneous catalysts such as microporous cation-exchange resins, it was evidence experimentally: (i) olefins that form secondary carbocations (e.g., *i*-Pr) generate predominantly ortho products; (ii) olefins that form tertiary carbocations (e.g., *t-Bu*) generate initially high ortho/para ratios but generate more para product at elevated temperature.

Calculated stabilities of various carbocations and alkylated phenols in the gas phase and in the phenol solution are summarized in Table 1. In three cases studied (i.e., ethyl, *i*-Pr, and *t*-Bu), para isomers of C-alkylated carbocations and the corresponding alkyl phenols are thermodynamically the most stable products. The stability of the O-alkylated ion increases from primary ($C_2H_5^+$) to secondary ($C_3H_7^+$) to tertiary ($C_4H_9^+$) alkyl cations, as the stability of the alkyl cation itself increases. The *o*-C-alkylphenols are in general more stable than the O-alkylphenols but less stable than the *p*-C-alkylphenols.

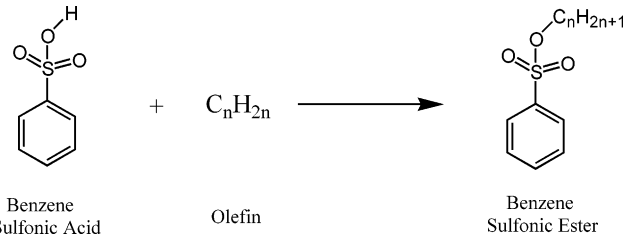

Figure 1. Formation of the sulfonic ester is a highly exothermic reaction.

3.3. The Neutral Pathway Mechanism.

At first, we noted that the reaction between olefin and the benzene sulfonic acid to form a benzene sulfonic ester is very exothermic (17.7 kcal/mol for *i*-Pr and 13.6 kcal/mol for *t*-Bu) and has virtually no transition barrier (Figure 1). Therefore we would expect the sulfonic ester to form irreversibly.

The next step involves interactions between the benzene sulfonic ester and phenol, a neutral mechanism. Three plausible reaction pathways, corresponding to *oxo*-, *o*-, and *p*-alkylations from the sulfonic ester, have been studied. Figure 2 depicts the reaction pathway for O-alkylation. The TS (TS1) for the direct *oxo*-alkylation (O-alkylation) reassembles a "six-ring" (S−O−H−O−R−O−S) with a transition barrier of 30.62 kcal/mol with respect to the sulfonic ester complex but is about 13 kcal/mol compared to the originally separated system that contains "phenol + *i*-Pr + acid". Once passing the TS1, it forms an intermediate H-bonded oxo configuration (*oxo*-LM1) followed by the separation of ether and acid to the catalyst regeneration. The overall reaction path is slightly endothermic with the reaction energy of 0.90 and 2.51 kcal/mol before and after the separation.

C-Alkylations (ortho and para) require an additional intermediate, the quinone formation. As indicated in Figure 3, the sulfonic ester complex first overcomes a transition state (TS2) to reach an intermediate *o*-quinone (*o*-quin) configuration, then continues by passing another transition state (TS4) to form the H-bonded *o*-alkylphenol (*o*-LM) complex followed by the separation process to regenerate acid-catalysts. The *o*-alkylation for *i*-propyl sulfonic ester has a transition barrier of 35.70 kcal/mol in TS2 and is exothermic of −4.13 kcal/mol before and −1.96 kcal/mol after the catalyst regeneration.

The *p*-alkylation (Figure 4) has a similar pathway to the *o*-alkylation. However, a reorientation of the sulfonic ester complex is required to reach TS3 such that the benzoic sulfonic ring is nearly perpendicular to the phonic ring. This gives rise to an addition of a ∼5.0 kcal/mol transition barrier for TS3 compared to TS2, leading *p*-alkylation to the highest reaction barrier in the neutral pathway.

The neutral pathway mechanism predicts a lower transition barrier for the O-alkylation compared to C-alkylations, indicating ether as the main product. This is in line with the experimental observations of an excess ether formation in the early reaction stage. However direct rearrangements among *oxo*-, *o*-, and *p*-alkyphenols in the neutral environment are energetic forbidden. The energies required for such rearrangements have been estimated to be ∼70 kcal/mol; loss of aromaticity of the benzene ring is responsible for these high barriers.

3.4. The Ionic Pathway Mechanism.

The homogeneously acid-catalyzed rearrangement of alkyl phenyl ethers to alkylphenols has been known for over a century.[49] Investigations showed that such rearrangement could lead to ring alkylations via both the intra- and intermolecular routes,[50−53] depending on the catalyst type and the reaction media homogeneity.[54] However, the situation is very different in heterogeneous catalysts, and reported results are contradictory. No evidence of the ether rearrangement is found when a heterogeneous silica-supported BF_3 catalyst was employed for such a reaction.[47] On the other hand, *o*- and *p*-alkylations with and without ether rearrangements[55] were reported for the heterogeneous Amberlyst-15 catalyst.

To provide a theory accountable for the alkyl phenyl ether rearrangement, we considered an ionic rearrangement mechanism. In this mechanism, migrations of the alkyl group occur in a positively charged environment resulted from protonation. The protonation/deprotonation energies (Table 2) are calculated from

$$\Delta E^{\mathrm{solv}}{}_{\mathrm{prot/deprot}} = \pm\{E^{\mathrm{solv}}(\mathrm{AH}^+) - E^{\mathrm{solv}}(\mathrm{A}) - E^{\mathrm{solv}}(\mathrm{H}^+)\}\ \text{(in solution)} \quad (1)$$

where $E^{\mathrm{solv}}(\mathrm{AH}^+)$ and $E^{\mathrm{solv}}(\mathrm{A})$ are calculated total energies of protonated and neutral configurations in solution (phenol in this case) and $E^{\mathrm{solv}}(\mathrm{H}^+)$ is the total free energy of proton in solution.

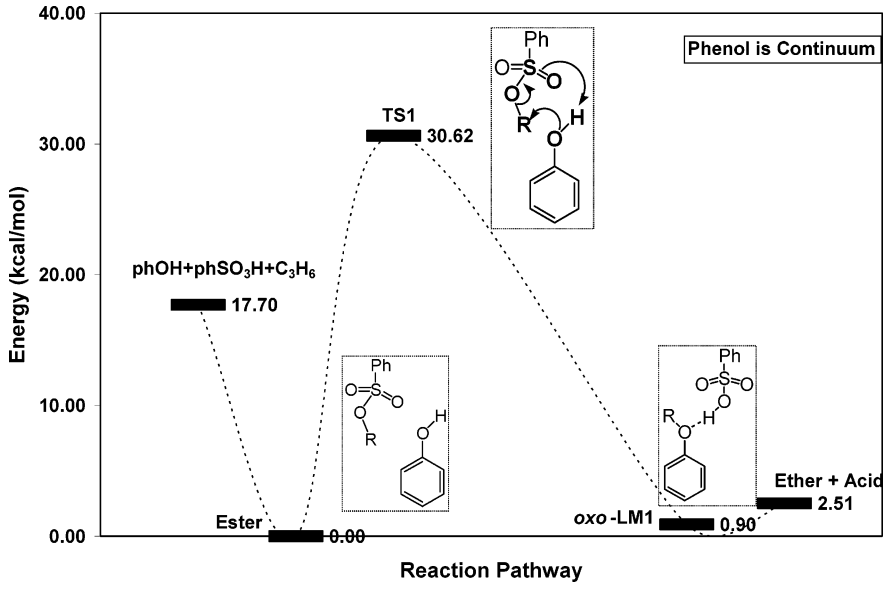

Figure 2. Reaction pathway for the direct O-alkylation.

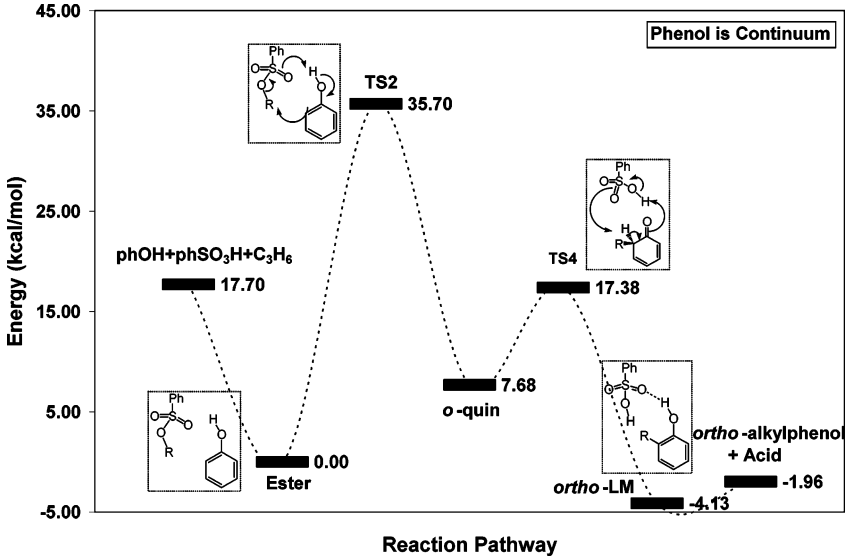

Figure 3. Reaction pathway for the direct *o*-C-alkylation.

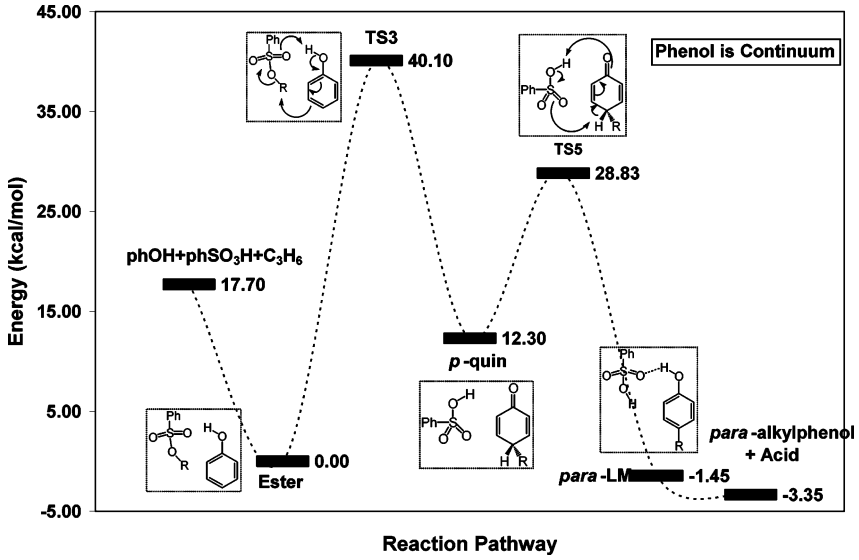

Figure 4. Reaction pathway for the direct *p*-C-alkylation.

TABLE 2: Calculated Protonation Energies of Ethers and Deprotonation Energies of Protonated *o*-C-alkylphenols and *p*-C-alkylphenols[a]

	protonation/deprotonation energies (kcal/mol)		
R	oxo	ortho	para
H	+9.26/−9.26	+6.13/−6.13	+0.24/−0.24
CH_3	+12.81/−12.81	+9.43/−9.43	+3.00/−3.00
C_2H_5	+11.31/−11.31	+9.06/−9.06	+6.15/−6.15
C_3H_7	+6.48/−6.48	**+11.32/−11.32**	+6.60/−6.60
C_4H_9	+2.54/−2.54	**+5.80/−5.80**	+5.82/−5.82

[a] The standard free solvation energy for a proton is taken as $E^{solv}(H^+) = 259 \pm 5$ kcal/mol.

Although the precise experimental value of $E^{solv}(H^+)$ remains uncertain, its range has been established between −254 to −261 kcal/mol.[56,57] A DFT calculation[58] at the same level of the present work for the standard free energies of H_2O(aq) and H_3O^+(aq) calculations found $E^{solv}(H^+) = -259.38$ kcal/mol after extracting the translational and rotational free energy contributions of −6.28 kcal/mol. Therefore we chose $E^{solv}(H^+) = 259 \pm 5$ kcal/mol.

Five possible protonated configurations (p-ether, p-ipso, p-ortho, p-meta and p-para) are shown and the migration paths

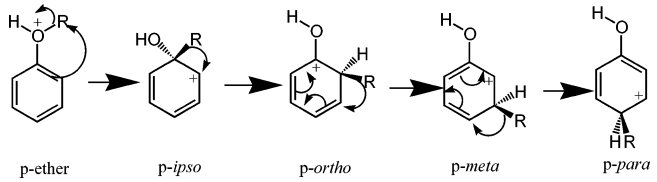

Figure 5. Five possible protonated configurations, p-ether, p-ipso, p-ortho, p-meta, and p-para, for migrations of the alkyl group in the ionic pathway.

of the alkyl group (R) from the p-ether to p-para configurations are also illustrated in Figure 5. For comparisons, five R groups (H, Me = CH_3, Et = C_2H_5, *i*-Pr = C_3H_7, and *t*-Bu = C_4H_9) are selected. The overall energetic diagram including all stable and transition states of the alkyl group's migration along various sites on the benzoic ring in the phenol solution is shown in Figure 7 with data listed in Table 3. Evidently, the overall migration pathway can be divided into two sections, from p-ether to p-ortho (section 1) and from p-ortho to p-para (section 2).

The size of R has more significant effects in section 1 than in section 2. The transition barrier of p-TS1 systematically decreases by ∼10 kcal/mol with the addition of one methyl group, e.g., ∼50 kcal/mol for H, ∼40 kcal/mol for CH_3, ∼30

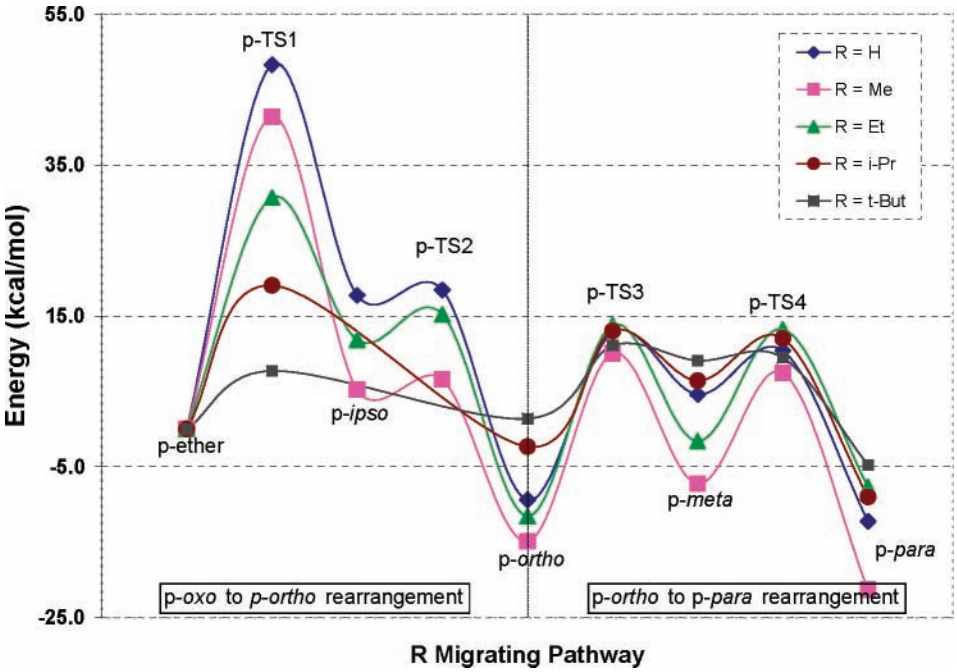

Figure 6. The energetic diagram of migrations of five different alkyl groups {H, methyl (Me), ethyl (Et), *iso*-propyl (*i*-Pr), and *tri*-butyl (*t*-Bu)} in the phenol solution. For each alkyl group, energies of four TSs (p-TS1, p-TS2, p-TS3, and p-TS4) along with five stable states (p-ether, p-ipso, p-ortho, p-meta, and p-para) are shown. All energies, in unit of kcal/mol, are referred to the protonated ether configuration (p-ether). Notice that the p-ipso configuration becomes unstable for large R groups (*iso*-protene and *tri*-butene).

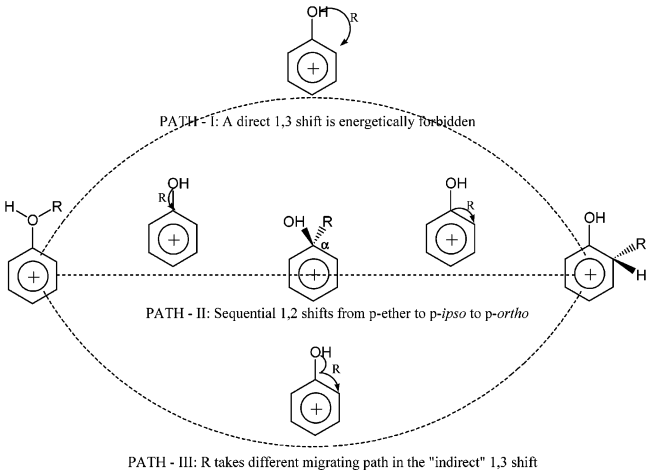

Figure 7. Different migrating paths for the alkyl R group from p-ether to p-ortho configurations.

kcal/mol for C_2H_5, ~20 kcal/mol for *i*-C_3H_7, and ~10 kcal/mol for *t*-C_4H_9. This feature suggests that the oxo/ortho migration is a steric hindrance driven effect, which determines the R selectivity in the ionic pathway mechanism.

The smaller R groups (H, CH_3, and C_2H_5) migrate from p-ether to p-ipso to p-ortho via sequential 1,2 shifts (PATH II, refer to Figure 7). In these cases, the R group attaching to the α-carbon forms a true intermediate state (an energetic stable state with no imaginary vibrations). But for R = *i*-Pr and *t*-Bu, the p-ipso configuration is no longer a stable intermediate due to the stronger steric hindrance effect. As a result of this, geometry optimization failed to locate a stable p-ipso configuration for *i*-Pr and *t*-Bu as they all ended up at the p-ortho state. Instead, R (*i*-pr and *t*-bu) takes an "indirect" 1,3 shift (PATH III, refer to Figure 7). This "indirect" 1,3 shift is different from the high transition barrier ordinary 1,3 shift (refer to Figure 7, PATH I with a transition barrier ≈ 40 kcal/mol) in the way that it is along the 1−2−3 path except for a firmly stay at the p-ipso state. The geometry of p-TS1 features the alkyl group located between of p-ether and p-ipso configurations.

TABLE 3: Energy Data as Shown in Figure 7[a]

	calculated relative energy (kcal/mol)					
	H					
configuration	6-31G(d)	lacvp**	Me	Et	*i*-Pr	*t*-Bu
p-ether	0.00	0.00	0.00	0.00	0.00	0.00
p-TS1	48.29	48.58	41.40	30.68	19.03	7.72
p-ipso	17.72	17.69	5.23	11.85	not stable	not stable
p-TS2	18.43	18.56	6.61	15.21	not stable	not stable
p-ortho	−9.41	−9.20	**−14.88**	**−11.53**	**−2.34**	**1.37**
p-TS3	12.82	12.92	10.02	13.81	13.01	11.06
p-meta	4.59	4.77	**−7.24**	**−1.61**	**6.42**	**9.09**
p-TS4	10.37	10.63	7.46	13.21	12.02	9.46
p-para	−12.23	−12.06	**−21.29**	**−7.67**	**−8.99**	**−4.76**

[a] To test the efficiency of the 6-31G(d) basis set, for the H cases, a larger basis set (lacvp**) has also been used. The energy differences are within ~0.2−0.3 kcal/mol.

The size of R also affects the stability of protonated states. The relative stable energies have the similar order of Me > Et > *i*-Pr > *t*-Bu at p-ortho, p-meta and p-para states (Table 3 in bold). Here again, we can see the steric hindrance effect between the alkyl group and the H-atom attaching on the same ring position. The R = H case falls out of this pattern because its different bonding nature with the benzoic ring (the C−H bond) than the rest alkyl groups (the C−C bond).

The ionic rearrangement mechanism is superior to the neutral mechanism because of significantly lower transition barriers. For example, the highest transition barrier for R = *i*-Pr to migrate from p-ether to the p-para state is 19.03 kcal/mol (refer to Table 3). Plus the protonation energy of 6.48 kcal/mol (Table 2), the overall energy barrier of 25.51 kcal/mol is much less than the neutral rearrangement. Advantages of ionic migrations are: (1) Protonated states are in nature unstable. Competition between the H atom and the R group can easily lead to either deprotonation or releasing of R for migration. (2) The addition of the H atom maintains aromaticity once R is "released". (3)

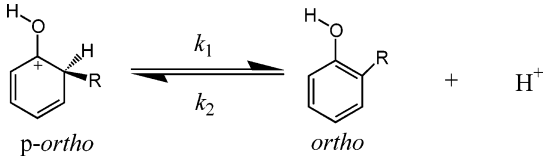

Figure 8. Breaking of the ionic pathway chain − the formation of final *o*-alkylphenol product from the protonated ortho state.

Only one "distorted" C−C bond (or C−H bond for R = H) needs to be broken.

3.5. Selectivity of C-Alkylations: the ortho/para Ratio.

The ionic mechanism, however, is not a straightforward pathway to the *p*-alklation. The R group at the p-ortho configuration might "kick-out" the H atom to form the final *o*-alklyphenol product (Figure 8). Since the deprotonation at the p-ortho configuration is an energetically favorable process (Table 2), *o*-alkylphenol becomes the predominant product in the early migrating processing.

The continuous migration from *o*-alkylphenol to *p*-alkylphenol is a thermodynamically driven process, since the later is energetically more stable (e.g., $E_{para} = -3.35$ and $E_{ortho} = -1.96$ kcal/mol for R = *i*-Pr, respectively, see Figures 3 and 4) and the transition barrier is substantially low ($E_{p-TS3} = 12.02$ kcal/mol for R = *i*-Pr, see Table 3) via the ionic pathway. Protonation of ortho to p-ortho (equilibrium constant k_2) is therefore an important factor in determining the final ortho/para ratio of C-alkylated products. For instance, our calculated deprotonation energies of *i*-Pr and *t*-Bu at the ortho configuration are −11.32 and −5.80 kcal/mol, respectively (Table 2, in bold), predicting a much higher *o/p* ratio for *i*-Pr over *t*-Bu. This is consistent with the experimental observation that olefins that form secondary carbocations generate predominantly ortho products and olefins that form tertiary carbocations generate initially high ortho/para ratio but generate more para product at elevated temperature.

The *p*-alkylation favors an acidic environment because the acidity (e.g., proton concentration) not only provides an easy entrance for the ionic pathway (from ether to p-ether) but also prevents from the early exit of the R migration (from p-ortho to ortho). In the aqueous solution, even a weak acid can generate enough amounts of the H^+ ion. For heterogeneous solid catalysts such as macroporous cation-exchange resin, the large excess of phenol used in most experiments serves as solvent. The acidity of catalysts might substantially be reduced when presented in the phenol solution compared to in the aqueous solution. For the catalytic system of our interest, i.e., the cation-exchange resin catalyst Amberlyst-15 modeled by the benzene sulfonic acid, we have calculated its pK_a values in both water and phenol solutions following the procedure as described in ref 58. The calculated pK_a = 1.08 in water is comparable with the experimental value of pK_a = 0.70, indicating a strong Lewis acid of the sulfonic acid. While in phenol, the benzene sulfonic acid becomes a relative weak acid with a calculated pK_a value of 3.91.

4. Discussions

We attempt here to provide a molecular level understanding of the complex chemistry happening in the phenol alkylation when an Amberlyst-15 type sulfonic acid resin catalyst is used. We proposed a combination of neutral and ionic multistep reaction pathway mechanism, which is summarized as follows:

1. The alkene first reacts with the sulfonic acid to form a sulfonic ester. This reaction is highly exothermic (17.7 kcal/mol for *i*-Pr and 13.6 for *t*-Bu).

2. Among three plausible neutral reaction pathways between the sulfonic acid ester and phenol that lead to direct O-alkylation, *o*-C-alkylation, and *p*-C-alkylaton, the ether formation is found to be the most energetic favorable. For R = *i*-Pr, the transition barrier is ∼30 kcal/mol. Barriers for the direct *o*-C-alkylation and *p*-C-alkylation are about 5 and 10 kcal/mol higher that of the O-alkylation. This result provides a theory accountable for the initial high ether concentration observed in most experiments.

3. Protonation significantly lowers barriers for rearrangements of the alkyl group between of various substitutive sites on the aromatic ring. The alkyl group migrates through a serial of the 1,2 shifts. The migration from p-ether to p-ortho is a steric hindrance driven process determining the R selectivity.

4. The protonated ortho configuration is a "pivot" point (circled, Figure 9). Competition between R and H at the substitutive size determines the ortho/para ratio of final C-alkylation products.

5. Acidity (the H^+ concentration) determines the selection of the neutral or ionic pathway and therefore controls the ortho/para ratio of final C-alkylation products.

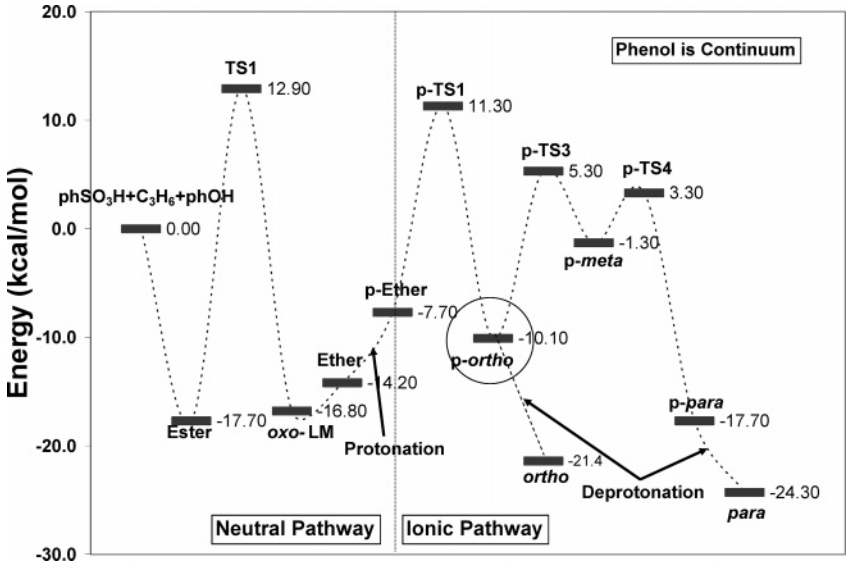

Figure 9. The overall phenol alkylation pathway with *iso*-propene catalyzed by the benzene sulfonic acid in the phenol solution.

The overall alkyhlation pathway of *i*-Pr is summarized in Figure 9. This multistep alkylation mechanism is consistent with the Attina et al. experimental observations[45] that the *tert*-butylation of phenol in gas phase occurred predominantly yielded the O-alkylated ether as the major product, since the neutral pathways are predominant in the gas-phase reaction. It also agrees with Campbell et al. results[55] that the C-alkylation follows an initial high concentration of the phenolic ether, where the ionic rearrangements occurred.

Acknowledgment. Financial support from ChevronTexaco is highly acknowledged. We would also like to thank all colleagues at the Power, Energy & Environmental Research Center (PEER) and Material and Processing Simulation Center (MSC) at Caltech for numerous helpful discussions. The computations were done mainly in MSC. The MSC is supported by grants from DoE, ASCI, ARO-MURI, ARO-DARPA, ONR-MURI, NIH, ONR, General Motors, ChevronTexaco, Seiko-Epson, Beckman Institute, and Asahi Kasei.

References and Notes

(1) Weissemel, K.; Arpe, H.-J. In *Industrial Organic Chemistry*, 3rd ed.; VCH Weinheim: 1997; p 358.

(2) Becke, A. D. *J. Chem. Phys.* **1993**, *98*, 5648; **1992**, *96*, 2155; **1992**, *97*, 9173.

(3) Lee, C.; Yang, W.; Parr, R. G. *Phys. Rev. B.* **1988**, *37*, 785.

(4) Miklis, P. C.; Ditchfield, R.; Spencer, T. A. *J. Am. Chem. Soc.* **1998**, *120*, 10482.

(5) Tannor, D. J.; Marten, B.; Murphy, R.; Friesner, R. A.; Sitkoff, D.; Nicholls, A.; Ringnalda, M. N.; Goddard, W. A., III; Honig, B. A. *J. Am. Chem. Soc.* **1994**, *116*, 11875.

(6) Honig, B.; Nicholls, A. *Science* **1995**, *268*, 1144.

(7) Marten, B.; Kim, K.; Cortis, C.; Friesner, R. A.; Murphy, R. B.; Ringnalda, M. N.; Sitkoff, D.; Honig, B. *J. Phys. Chem.* **1996**, *100*, 11775−11788.

(8) Nicholls, A.; Honig, B. *J. Comput. Chem.* **1991**, *12*, 435.

(9) (a) Jaguar 3.5; Schrödinger Inc. Portland, OR, 1998. (b) Greeley, B. H.; Russo, T. V.; Mainz, D. T.; Friesner, R. A.; Langlois, J.-M.; Goddard, W. A., III.; Donnolly, R. E.; Ringgnalda, M. N. *J. Chem. Phys.* **1994**, *101*, 4028.

(10) (a) Cacace, F. *Pure Appl. Chem.* **1997**, *69*, 227. (b) Cacace, F. *Spec. Publ. − R. Soc. Chem.* **1995**, *148*, 235. (c) Cacace, F.; Crestoni, M. E.; Fornarini, S. *J. Am. Chem, Soc.* **1992**, *114*, 6776. (d) Attina, M.; Cacace, F.; Ricci, A.; *J. Am. Chem. Soc.* **1991**, *113*, 5937. (e) Cacace, F. *Acc. Chem. Res.* **1988**, *21*, 1, 215.

(11) Kuck, D. *Mass Spectrom. Rev.* **1990**, *9*, 583.

(12) (a) DePuy, C. H.; Gareyev, R.; Fornarini, S. *Int. J. Mass Spectrom. Ion Processes* **1997**, *161*, 41. (b) Chiavarino, B.; Crestoni, M. E.; DePuy, C. H.; Fornarini, S.; Gareyev, R. *J. Phys. Chem.* **1996**, *100*, 16201. (c) Crestoni, M. E.; Fornarini, S. *J. Am. Chem. Soc.* **1994**, *116*, 5873. (d) Cerichelli, G.; Crestoni, M. E.; Fornarini, S. *J. Am. Chem. Soc.* **1992**, *114*, 2002.

(13) Steinberg, H.; Sixma, F. L. J. *Recl. Trav. Chim. Pays-Bas* **1962**, *81*, 185.

(14) (a) Brouwer, D. M.; Mackor, E. L.; Maclean, C. In *Carbonium Ions*; Olah, G. A., Schleyer, P. v. R., Eds.; Wiley: New York, 1970; Vol. 2, Chapter 20. (b) Brouwer, D. M. *Recl. Trav. Chim. Pays-Bas* **1968**, *87*, 611.

(15) (a) Meier, B. H.; Ernst, R. R. *J. Am. Chem. Soc.* **1979**, *101*, 6441. (b) Koptyug, V. A. *Top. Curr. Chem.* **1984**, *122*, 1. (c) Saunders, M. In *Magnetic Resonance in Biological Systems*; Erhenberg, A., Malmstrom, B. G., Vanngerd, T., Eds.; Pergamon: Oxford, 1967.

(16) Berthomieu, D.; Brenner, V.; Ohanessian, G.; Denhez, J. P.; Millié, P.; Audier, H. E. *J. Phys. Chem.* **1995**, *99*, 712.

(17) Dewar, M. J. S.; Dieter, K. M. *J. Am. Chem. Soc.* **1986**, *108*, 8075.

(18) Heidrich, D.; Geimmer, M.; Sommer, B. *Tetrahedron* **1976**, *32*, 2027.

(19) (a) Gleghorn, J. T.; McConey, F. W.; Lundy, K, *J. Chem. Res. Synop.* **1978**, *418*. (b) Gleghorn, J. T.; McConey, F. W. *J. Chem. Soc., Perkin Trans.* **1976**, *2*, 1078.

(20) Effenberger, F.; Reisinger, F.; Schönwälder, K. H.; Bäuerle, P.; Stezowski, J. J.; Jogun, K. H.; Schollköpf, K.; Stohrer, W.-D. *J. Am. Chem. Soc.* **1987**, *109*, 882.

(21) (a) Devlin, J. L., III; Wolf, J. F.; Taft, R, W.; Hehre, W. J. *J. Am. Chem. Soc.* **1976**, *98*, 1990. (b) Wolf, J. F.; Devlin, J. L., III.; DeFrees, D. J.; Taft, R. W.; Hehre, W. *J. Am. Chem. Soc.* **1976**, *98*, 5097.

(22) Schleyer, P.v. R.; Buzek, P.; Muller, T.; Apeloig, Y.; Seihl, H.-U. *Angew. Chem., Int. Ed. Engl.* **1993**, *32*, 1471.

(23) McAdoo, D. *J. Mass Spectrom. Rev.* **1988**, *7*, 363.

(24) Hammerum, S. *J. Chem. Soc. Chem. Commun.* **1988**, 858.

(25) Bowen, R. D. *Acc. Chem. Rev.* **1991**, *24*, 363.

(26) Longevialle, P. *Mass Spectrom. Rev.* **1992**, *11*, 157.

(27) Morton, T. H. *Org. Mass. Spectrom.* **1992**, *16*, 423.

(28) (a) Dewar, M. J. S. *J. Chem. Soc.* **1946**, *406*, 777. (b) Dewar, M. J. S. *The Electronic Theory of Organic Chemistry*; Oxford University Press: London, 1949.

(29) (a) Olah, G. A.; Kuhn, S. F.; Flood, S.; Evans, J. C. *J. Am. Chem. Soc.* **1961**, *83*, 4571. (b) Olah, G. A. *Acc. Chem. Res.* **1971**, *4*, 240. (c) Olah, G. A.; Lin, H. C. *J. Am. Chem. Soc.* **1974**, *96*, 2892.

(30) Dougherty, D. A. *Science* **1996**, *271*, 163.

(31) Ma, J. C.; Dougherty, D. A. *Chem. Rev.* **1997**, *97*, 1303.

(32) (a) Poulter, C. D.; Rilling, H. C. *Acc. Chem. Res.* **1978**, *11*, 307. (b) Abe, I.; Rohmer, M.; Prestwich, G. D. *Chem. Rev.* **1993**, *93*, 2189. (c) Hirage, Y.; Ito, D. I.; Sayo, T.; Ohta, S.; Suga, T. *J. Am. Chem. Soc., Chem. Commun.* **1994**, 1057.

(33) (a) Kochi, J. K. *Adv. Phys. Org. Chem.* **1994**, *29*, 185. (b) Shelly, K.; Finster, D. C.; Lee, Y. J.; Scheidt, W. R.; Reed, C. A. *J. Am. Chem. Soc.* **1985**, *107*, 5955.

(34) Bauschlicher, C. W., Jr.; Partridge, M.; Langhoff, S. R. *J. Phys. Chem.* **1992**, *96*, 3273.

(35) Roszak, S.; Balasubramaniam, K. *Chem. Phys. Lett.* **1995**, *234*, 101.

(36) Kearney, P. C.; Mizoue, L. S.; Kurmf, R. A.; Forman, J. E.; McCurdy, A.; Dougherty, D. A. *J. Am. Chem. Soc.* **1993**, *115*, 9907.

(37) Kim, K. S.; Lee, J. Y.; Lee, S. J.; Ha, T.-K.; Kim, D. H. *J. Am. Chem. Soc.* **1994**, *116*, 7399.

(38) Mecozzi, S.; West, A. P., Jr.; Dougherty, D. A.*J. Am. Chem. Soc.* **1996**, *118*, 2307.

(39) Mecozzi, S.; West, A. P., Jr.; Dougherty, D. A. Proc. *Natl. Acad. Sci. U.S.A.* **1996**, *93*, 10566.

(40) (a) Grüzamacher, H. F.; Filges, U. *Org. Mass. Spectrom.* **1986**, *21*, 673. (b) Bäther, W.; Kuck, D.; Grüzamacher, H. F.; *Org. Mass Spectrom.* **1985**, *20*, 572. (c) Bäther, W.; Grüzamacher, H. F. *Int. J. Mass Spectrom. Ion Phys.* **1985**, *64*, 193.

(41) Gonzalo, T. S. *Ann. Chim.* **1983**, *79*, 486.

(42) (a) Hehre, W. J.; Pople, J. A. *J. Am. Chem. Soc.* **1972**, *94*, 6091. (b) Hehre, W. J.; Radom, L.; Schleyer, P.v. R.; Pople, J. A. *Ab Initio Molecular Orbital Theory*; John Wiley and Sons: New York, 1986; p. 396. (c) Sieber, S.; Schleyer, P.v. R.; Gauss, J. *J. Am. Chem. Soc.* **1993**, *115*, 6987. (d) Glukhovtsev, M. N.; Pross, A.; Nicolaides, N.; Radom, L. *J. Chem. Soc., Chem. Commun.* **1995**, 2347.

(43) Takahashi, Y.; Sankararaman, S.; Kochi, J. K. *J. Am. Chem. Soc.* **1989**, *111*, 2954.

(44) Berthomieu, D.; Brenner, V.; Ohanessian, G.; Denhez, J. P.; Millié, P.; Audier, H. E. *J. Am. Chem. Soc.* **1993**, *115*, 2505.

(45) Attina, M.; Cacace, F.; Ciranni, G.; Giacomello, P. *J. Chem. Soc. Chem. Commun.* **1976**, 466.

(46) Kim, S. D.; Lee, K. H. *J. Mol. Catal.* **1993**, *78*, 237

(47) Wilson, K.; Adams, D. J.; Rothenberg, G.; Clark, J. H. *J. Mol. Catal. A.* **2000**, *159*, 309.

(48) Dowbenko, R. In *Kirk-Othmer Encyclopedia of Chemical Technology*; Kroschwitz, J. J., Howe-Grant, M., Eds.; Wiley: New York, 1992; Vol. 2, p 106.

(49) Hartmann, C.; Gatterman, L. *Chem. Ber.* **1892**, *25*, 2531.

(50) Smith, R. A. *J. Am. Chem. Soc.* **1933**, *55*, 849.

(51) Smith, R. A. *J. Am. Chem. Soc.* **1934**, *56*, 717.

(52) Shine, H. J. In *Aromatic Rearrangement*; Eaborn, C., Chapman, N. B., Eds.; Elsevier: Amsterdam, 1967; p 82.

(53) Sartori, G.; Bigi, F.; Maggi, R.; Arienti, A. *J. Chem. Soc., Perkin. Trans.* **1997**, *1*, 257.

(54) Dewar, M. J. S. In *Molecular Rearrangements*; de Mayo, P. Ed.; Wiley, New York, 1963; p 306.

(55) (a) Santacesaria, E.; Silvani, R.; Wilkinson, P.; Carra, S. *Ind. Eng. Chem. Res.* **1988**, *27*, 57. (b) Campbell, C. B.; Onopchenko, A.; Young, D. C. *Ind. Eng. Chem. Res.* **1990**, *29*, 642.

(56) Lim, C.; Bashford, D.; Karplus, M. *J. Phys. Chem.* **1991**, *95*, 5610−5620.

(57) Reiss, H.; Heller, A. *J. Phys. Chem.* **1985**, *89*, 4207−4213.

(58) Jang, Y. H.; Sowers, L. C.; Cağin; Goddard, W. A., III. *J. Phys. Chem. A* **2001**, *105*, 274−280.